

Gate Field Induced Bandstructure and Mobility Variations in p-type Silicon Nanowires

Neophytos Neophytou and Hans Kosina

Institute for Microelectronics, TU Wien, Gußhausstraße 27-29/E360, A-1040 Wien, Austria
e-mail: {neophytou|kosina}@iue.tuwien.ac.at

1. Abstract

The bandstructure of p-type Si nanowires (NWs) is calculated self-consistently using the $sp^3d^5s^*$ -spin-orbit-coupled (SO) atomistic tight-binding (TB) model and the 2D Poisson equation. The Boltzmann transport formalism is then used for calculation of the low-field mobility. We show that the bandstructures of the [110] and [111] NWs change as the channel is driven into inversion, which causes a ~50% increase in the phonon-limited hole mobility. For short channel MOSFET devices, however, the total mobility is lower because it is affected by the so called “ballistic” mobility.

2. Approach

Silicon NWs have recently attracted significant attention as candidates for high performance transistor channels [1, 2]. Low-dimensional materials offer the capability of improved performance due to additional geometrical degrees of freedom in engineering their dispersions such as the cross section size and orientation, especially for p-type NWs [3]. In this work, we show that electrostatic carrier confinement through gating can also introduce dispersion variations in p-type NWs and influence their transport properties. We calculate the phonon-limited, low-field mobility in NWs of diameter $D=12\text{nm}$ (~5500 atoms in the unit cell) in the [100], [110] and [111] transport orientations. We use the $sp^3d^5s^*$ -SO TB model for the electronic structure, self-consistently coupled to the 2D Poisson equation [4], as shown in Fig. 1. Upon convergence, the mobility is extracted using linearized Boltzmann transport theory [3].

3. Results

Figure 2 shows the hole injection velocity and ballistic on-current for p-type NWs of $D=8\text{nm}$. This is a typical result from the first three steps of the simulation procedure in Fig. 1. A large anisotropy is observed. The [111] NW shows the best performance, whereas the [100] NW is the worst. The model captures the charge distribution in the cross section of the NW as shown in Fig. 3 for a [111] NW of $D=12\text{nm}$. The carrier density is

centered in the middle of the channel under low bias conditions (Fig. 3a), and shifts towards the surface at inversion conditions as expected (Fig. 3b). This electrostatic confinement causes strong variations in the dispersion of the NW. Figure 4a shows the dispersion under low bias conditions and Fig. 4b in inversion. As the holes are confined on the surface, the dispersion acquires lighter subbands, similar to what is observed under structural cross section confinement [3]. The same is observed for the [110] NW, but not for the [100] NW, and has consequences in the mobility versus gate bias (V_G) dependence as shown in Fig. 5. The lighter subbands cause the mobility to increase almost by ~50% with increasing V_G . At stronger inversion, however, the mobility decreases because at higher energies heavier subbands participate in transport (Fig. 4b).

For short channel, semi-ballistic transistors, however, the diffusive mobility definition loses its validity. The measured mobility is better explained by the combination of the diffusive and the so called “ballistic” mobility defined as $\mu_B=L_G/C_{OX}(V_G-V_T)R_{CH}$ [5]. The μ_B is shown in Fig. 6 versus V_G . Its magnitude is lower than the diffusive mobility in Fig. 5, and its trend different. The “ballistic” mobility will be more relevant for short channels, whereas the diffusive mobility for long channels. This is demonstrated in Fig. 7, which shows the total mobility (so called “apparent”) at inversion conditions ($V_G=-0.6\text{V}$ and -1V) versus channel length L_G . For longer channels, the mobility approaches the diffusive mobility values (peaks of Fig. 5), whereas as the channels shortens, it approaches the “ballistic” mobility values (of Fig. 6).

4. Conclusions

The $sp^3d^5s^*$ -SO atomistic tight-binding model is self-consistently coupled to Poisson equation and linearized Boltzmann transport for the calculation of mobility in silicon NWs. We show that the phonon-limited low-field mobility in p-type [110] and [111] NWs has a strong gate bias dependence and can increase by ~50% as the channel is driven into inversion. For short channel devices, however, the “apparent” mobility is influenced by the “ballistic” mobility, and it is lower.

References

- [1] K. H. Cho *et al.*, Appl. Phys. Lett., 92, 052102, 2008. [2] S. Bangsaruntip *et al.*, IEDM 2009, p. 297. [3] N. Neophytou and H. Kosina, PRB, 84, 085313, 2011. [4] N. Neophytou *et al.*, IEEE TED, 55, 1286, 2008. [5] N. Neophytou, T. Rakshit, and M. Lundstrom, IEEE TED, 56, 1377, 2009.

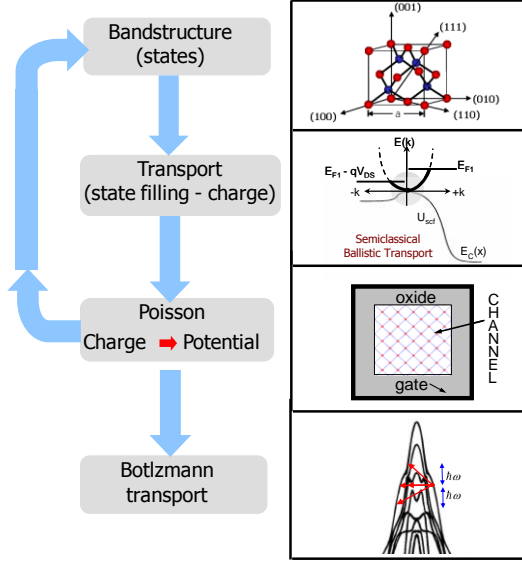


Fig.1: (a) Simulation procedure. The NW bandstructure is calculated using the $sp^3d^5s^*$ -SO TB model. (b) A semiclassical ballistic model is used to calculate the charge distribution in the NW. (c) The charge is self-consistently coupled to a 2D Poisson equation for the electrostatic potential in the cross section of the wire. From here, ballistic characteristics can be extracted. (d) Upon convergence (and at $V_D=0V$), Boltzmann transport theory is used for mobility calculations. (Relevant valence band scattering mechanisms are shown.)

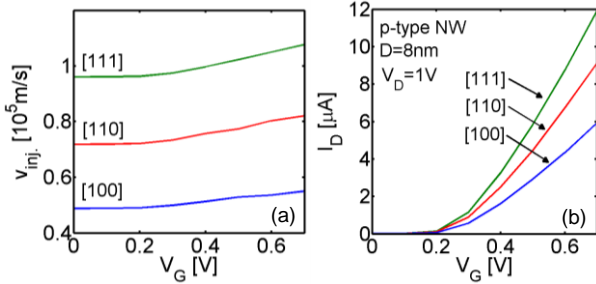


Fig.2: Ballistic injection velocity (a) and on-current (b) for p-type NWs of $D=8nm$, in the [100], [110] and [111] transport orientations.

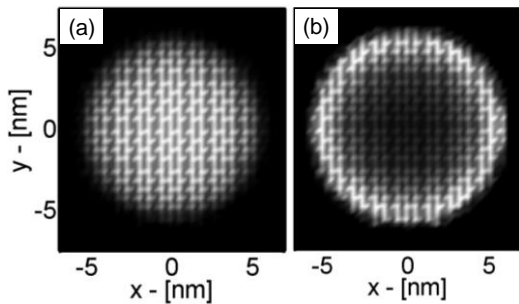


Fig.3: The hole distribution in the cross section of the [111] NW of $D=12nm$, at (a) off-state, and (b) on-state ($V_G=-0.8V$).

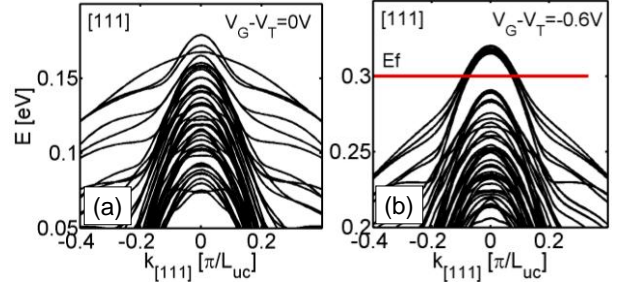


Fig.4: Dispersions of the [111] NW of $D=12nm$ for different gate bias conditions. (a) At $V_G=-0.2V$ the dispersion is close to its equilibrium shape. (b) At $V_G=-0.8V$ the channel is in inversion and the dispersion changes. The threshold voltage $V_T=-0.2V$.

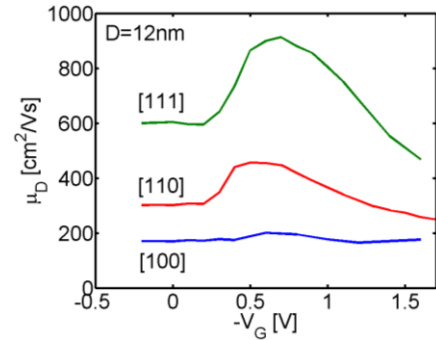


Fig.5: Phonon-limited low-field hole mobility for NWs of $D=12nm$ in the [100], [110], and [111] transport orientations versus gate bias ($-V_G$).

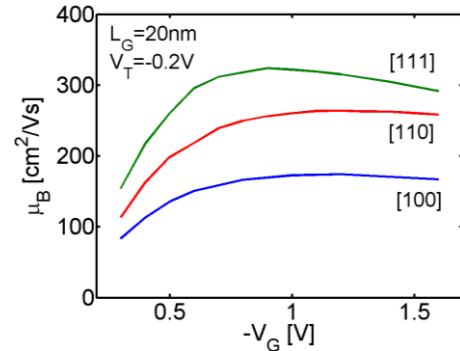


Fig.6: Hole "ballistic" mobility for NWs of $D=12nm$ in the [100], [110], and [111] transport orientations versus ($-V_G$). A device with channel length $L_G=20nm$ is assumed.

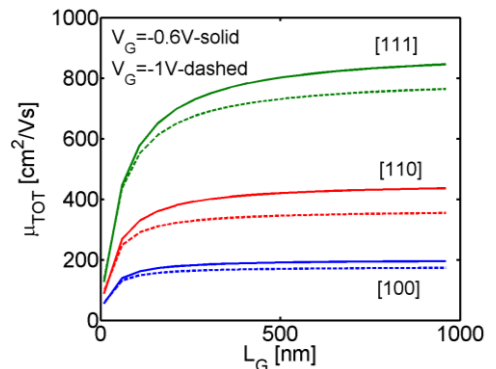


Fig.7: Total hole "apparent" mobility for NWs of $D=12nm$ in the [100], [110], and [111] transport orientations versus channel length L_G . V_G cases $V_G=-0.6V$ and $-1V$ are shown.